Scattering of Millimeter Waves by Metallic Strip Gratings on an Optically Plasma-Induced Semiconductor Slab

Kazuo Nishimura, *Student Member, IEEE,* and Makoto Tsutsumi, *Member, IEEE*

Abstract— **This paper presents the scattering characteristics of a TE electromagnetic plane wave by metallic strip gratings on an optically induced plasma slab in silicon at millimeter-wave frequencies. The characteristics were analyzed by using the spectral domain Galerkin method and estimated numerically. We examined how to control the resonance anomaly by changing the optically induced plasma density for metallic strip grating structures fabricated on highly resistive silicon. The optical control characteristics of the reflection and the forward scattering pattern of the grating structures were measured at Q band and are discussed briefly with theory.**

I. Introduction

ELECTRON-HOLE pairs in a semiconductor were induced optically by a light with photon energy that was greater than the semiconductor's band gap energy. We used this phenomena to control the millimeter waves in semiconductor waveguides, and this also has applications in antennas, high-speed switches, phase shifters, modulators, and filters [1], [2]. The control of millimeter waves in guided-wave systems poses some problems, such as greater losses, smaller physical dimensions, difficulty with input matching, and higher manufacturing costs inherent in higher frequencies. These difficulties are overcome by using quasioptical circuits that are large and do not need external contacts, which could interfere with millimeter-wave transmission, and by decreasing the thickness of the substrate to reduce the losses.

Previously, the reflection and transmission of millimeter waves from an optically induced plasma in a semiconductor were studied as a means of optically controlling of millimeter waves in a quasioptical system [3]. The optical control characteristics of millimeter waves performed by that method were inefficient. To enhance the efficiency of the optical control of millimeter waves, a *nipi*-doped semiconductor slab was recently demonstrated [4]. Millimeter-wave diffraction by a photo-induced plasma grating has also been studied for applications using an optically controllable quasioptical antenna, since the grating parameters, such as periodicity and plasma strip width, can easily be changed by the illumination pattern [5]. We have theoretically and experimentally investigated the scattering characteristics of a TM electromagnetic plane wave by metallic strip gratings on the optically induced plasma in a semiconductor at Q band [6]. These quasioptical systems, with their periodic structures, will enhance the effect of optical control. A resonance anomaly caused by the coupling of propagating diffracted waves with the mode of the waveguide was observed. The propagation characteristics of TE surface waves in an image line are equivalent to those of TE surface waves in a dielectric waveguide with a thickness that is twice that of the image line. The plasma with higher density changes the ungrounded semiconductor slab waveguide into a grounded semiconductor slab waveguide [1]. Therefore, the optically induced plasma in the semiconductor slab waveguide will have a greater effect on the propagation characteristics of a TE surface wave than those of a TM surface wave.

In this paper, we analyze the scattering characteristics of a TE electromagnetic plane wave by metallic strip gratings on the optically induced plasma in a semiconductor slab, using the spectral domain Galerkin method. We experimentally verify the optical control characteristics of the reflection and the forward-scattering patterns using two types of metallic strip gratings, fabricated on a high-resistance silicon wafer, at Q band.

Manuscript received January 23, 1996; revised August 26, 1996.

The authors are with the Faculty of Engineering and Design, Kyoto Institute of Technology, Kyoto-shi, 606, Japan.

Publisher Item Identifier S 0018-9480(96)08514-6.

II. Theory

A. Relative Complex Permittivity of the Optically Induced Plasma in the Semiconductor

The relative complex permittivity of the optically induced plasma region in the semiconductor is given by

$$\varepsilon_p = \varepsilon_s - \sum_{i=e,h} \frac{\omega_{pi}^2}{\omega^2 + \nu_i^2}\left(1 + j\frac{\nu_i}{\omega}\right) \tag{1}$$

where ε_s is the relative permittivity of the semiconductor without the plasma and $\nu_e(\nu_h)$ is the collision angular frequency for electrons (holes). ω is the angular frequency of millimeter waves and ω_{pi} is the plasma frequency. The plasma frequency can be expressed as

$$\omega_{pi}^2 = \frac{n_p e^2}{m_i^* \varepsilon_0} \qquad (i = e, h)$$

where n_p is the plasma density, e is the electronic charge, $m_i^*(i = e, h)$ is the effective mass of electrons/holes, and ε_0 is the free-space permittivity [1].

B. Spectral Domain Galerkin Method [6]–[9]

The metallic strip gratings, which are placed on an optically induced plasma semiconductor slab, are illustrated in Fig. 1. The thickness of the semiconductor and the optically induced

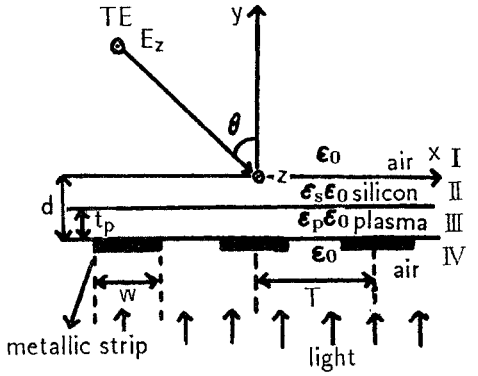

Fig. 1. Geometry of a metallic strip grating on the optically induced plasma silicon slab and TE wave incidence.

plasma are d and t_p. The light illumination from the region IV (the lower side with metallic strip gratings) induces the plasma not only in the silicon region between the metallic strips, but also in the silicon region beneath the metallic strips, because of plasma diffusion and light diffraction into the silicon region. Although the plasma distribution has a periodic variation along x and is nonuniform with y in the layer, to simplify the analysis of the grating structures we assumed the plasma was uniformly induced in region III of the semiconductor slab. The metallic strips have a surface resistance $R[\Omega]$, width w, and the periodicity of the gratings is T. The thickness of the strip is ignored. The electromagnetic field distribution is, by assumption, uniform in z direction $(\partial/\partial z = 0)$. We analyzed the scattering characteristics when the metallic strip gratings are illuminated by a TE electromagnetic plane wave (H_x^i, H_y^i, E_z^i) with an angle of incidence θ. The incident wave is described by

$$H_x^i = -\frac{\cos\theta}{Z_0} e^{-jk_0(\sin\theta x - \cos\theta y)}$$
$$E_z^i = e^{-jk_0(\sin\theta x - \cos\theta y)} \tag{2}$$

where k_0 is the free-space wavenumber and Z_0 is the free-space intrinsic impedance.

Next, we defined a Fourier transform pair as

$$A(x) = \frac{1}{2\pi}\int_{-\infty}^{\infty} \tilde{A}(k_x) e^{-jk_x x}\, dk_x$$
$$\tilde{A}(k_x) = \int_{-\infty}^{\infty} A(x) e^{jk_x x}\, dx. \tag{3}$$

The current distribution $J_z(x)$ on the metallic strip gratings satisfies the periodicity relation

$$J_z(x + nT) = J_z(x) e^{-jk_0 nT\sin\theta} \qquad n = 0, \pm 1, \pm 2, \pm 3, \cdots. \tag{4}$$

The electromagnetic field scattered by the metallic strip gratings are

$$H_x^s(x,y) = \frac{y}{|y|}\sum_{n=-\infty}^{\infty} \tilde{J}_z(\beta_n)\frac{\gamma_{In}\tilde{G}(\beta_n, y)}{jT} e^{-j\beta_n x} \tag{5}$$

$$E_z^s(x,y) = \sum_{n=-\infty}^{\infty} \tilde{J}_z(\beta_n)\frac{Z_0 k_0 \tilde{G}(\beta_n, y)}{jT} e^{-j\beta_n x} \tag{6}$$

where $\tilde{J}_z(\beta_n)$ is the Fourier transform of $J_z(x)$, and $\tilde{G}(\beta_n, y)$ is the Green's function in the spectral domain. $\tilde{J}_z(\beta_n)$ and $\tilde{G}(\beta_n, y)$ are given by

$$\tilde{J}_z(\beta_n) = \int_{-(w/2)}^{w/2} J_z(x) e^{j\beta_n x}\, dx \tag{7}$$

$$\tilde{G}(\beta_n, y) = \frac{e^{-j\gamma_{In}|y+d|}}{j2\gamma_{In}} \begin{Bmatrix} T_{\|}^-(\beta_n) \\ 1 + \Gamma_{\|}^-(\beta_n) \end{Bmatrix} \begin{matrix} y \geq 0 \\ y \leq -d \end{matrix} \tag{8}$$

$$\Gamma_{\|}^-(\beta_n) = \frac{\gamma_{In} - jC^-(\beta_n)}{\gamma_{In} + jC^-(\beta_n)}$$
$$T_{\|}^-(\beta_n) = \gamma_{In}\frac{\{1 - \Gamma_{\|}^-(\beta_n)\}}{je_n^-} e^{j\gamma_{In}d} \tag{9}$$

where

$$C^-(\beta_n) = \frac{e_n^-}{d_n^-},$$
$$d_n^- = b_n^- \cos\gamma_{IIIn} t_p - c_n^- \frac{\sin\gamma_{IIIn} t_p}{\gamma_{IIIn}}$$
$$e_n^- = b_n^- \gamma_{IIIn} \sin\gamma_{IIIn} t_p + c_n^- \cos\gamma_{IIIn} t_p,$$
$$b_n^- = \cos\gamma_{IIn}(d - t_p) + j\gamma_{In}\frac{\sin\gamma_{IIn}(d - t_p)}{\gamma_{IIn}}$$
$$c_n^- = \gamma_{IIn}\sin\gamma_{IIn}(d - t_p) - j\gamma_{In}\cos\gamma_{IIn}(d - t_p)$$
$$\gamma_{In} = \sqrt{k_0^2 - \beta_n^2}, \quad \gamma_{IIn} = \sqrt{\varepsilon_s k_0^2 - \beta_n^2}$$
$$\gamma_{IIIn} = \sqrt{\varepsilon_p k_0^2 - \beta_n^2}, \quad \beta_n = k_0\sin\theta + \frac{2\pi n}{T} \tag{10}$$

where $\Gamma_{\|}^-$ and $T_{\|}^-$ are the reflection and transmission coefficients of a TE electromagnetic plane wave from region IV, without the metallic strip gratings.

For this paper, we considered the resistive boundary condition to be the boundary condition on the metallic strip [7], [9]. The boundary condition is represented by

$$E_z^s(x, y = -d) + E_z^t(x, y = -d) = RJ_z(x) \quad \text{on the metallic strips} \tag{11}$$

$$E_z^t(x,y) = T_{\|}^+(k_0\sin\theta) e^{-jk_0(\sin\theta x - \cos\theta y)} \tag{12}$$

where E_z^t denotes the transmitted wave without metallic strip gratings. When we substitute (6), (8), and (12) into (11), we obtained the following integral equation for the current distribution on the metallic strip:

$$\frac{R}{Z_0}J_z(x) + \sum_{n=-\infty}^{\infty} \tilde{J}_z(\beta_n)\frac{k_0[1 + \Gamma_{\|}^-(\beta_n)]}{2T\gamma_{In}} e^{-j\beta_n x} = \frac{T_{\|}^+(k_0\sin\theta)}{Z_0} e^{-jk_0(\sin\theta x + \cos\theta d)} \tag{13}$$

where $T_{\|}^+$ is the transmission coefficients of a TE electromagnetic plane wave from region I without the metallic strip gratings. $T_{\|}^+$ was obtained by interchanging ε_s and ε_p, $(d - t_p)$ and t_p in (9) and (10). The surface current $J_z(x)$ is expanded in series with unknown coefficients I_m [8]

$$J_z(x) = e^{-jk_0\sin\theta x}\sum_{m=1}^{M} I_m \Phi_m(x) = \frac{1}{T}\sum_{m=1}^{M}\sum_{n=-\infty}^{\infty} I_m \check{\Phi}_m(n) e^{-j\beta_n x}$$

$$\Phi_m(x) = \begin{cases} (-j)^{m-1} \dfrac{\cos\dfrac{(m-1)\pi}{w}\left(\tilde{x}+\dfrac{w}{2}\right)}{\sqrt{1-\left(\dfrac{2\tilde{x}}{w}\right)^2}} & |\tilde{x}| \le \dfrac{w}{2} \\ 0 & \text{otherwise} \end{cases}$$

$$\tilde{x} = x - \nu T, \qquad (\nu = 0, \pm 1, \pm 2, \cdots, \cdots)$$

$$\frac{\tilde{\Phi}_m(n)}{w} = \frac{1}{w}\int_{-(w/2)}^{w/2} \Phi_m(x) e^{jn(2\pi/T)x}\, dx$$

$$= \frac{\pi}{4}\left\{ J_0\left(n\frac{w}{T} + (m-1)\frac{\pi}{2}\right) + (-1)^{m-1} J_0\left(n\frac{w}{T} - (m-1)\frac{\pi}{2}\right)\right\} \tag{14}$$

where $\Phi_m(x)$ is the current basis function and $J_0(x)$ denotes the zero order Bessel function. By substituting (14) into (13) and multiplying both sides of the result by $(\Phi_l^*(x)/w)e^{jk_0 \sin\theta x}$, and then integrating through the entire strip, the following system of linear equations were obtained:

$$[Z][I] = [V], \tag{15}$$

$$Z_{lm} = \frac{w}{T}\sum_{n=-\infty}^{\infty}\left[\frac{R}{Z_0} + \frac{k_0\{1+\Gamma_{\parallel}^{-}(\beta_n)\}}{2\gamma_{In}}\right] \cdot \frac{\tilde{\Phi}_l^*(n)}{w}\frac{\tilde{\Phi}_m(n)}{w}$$

$$V_l = \frac{T_{\parallel}^{+}(k_0 \sin\theta)}{Z_0} e^{-jk_0 \cos\theta d}\frac{\tilde{\Phi}_l^*(0)}{w}. \tag{16}$$

I_m was obtained by solving (15) numerically; the surface current was determined from (14). The scattered electromagnetic field was obtained from (5) and (6) [7], [8]. The transmission and reflection coefficients for the individual modes are defined by [7]

$$R_n = \frac{\dfrac{1}{2T}\mathrm{Re}\displaystyle\int_0^T (\boldsymbol{E}_n^r \times \boldsymbol{H}_n^{r*})\cdot \boldsymbol{y}\, dx}{\dfrac{1}{2T}\mathrm{Re}\displaystyle\int_0^T (\boldsymbol{E}^i \times \boldsymbol{H}^{i*})\cdot(-\boldsymbol{y})\, dx}$$

$$T_n = \frac{\dfrac{1}{2T}\mathrm{Re}\displaystyle\int_0^T (\boldsymbol{E}_n^t \times \boldsymbol{H}_n^{t*})\cdot(-\boldsymbol{y})\, dx}{\dfrac{1}{2T}\mathrm{Re}\displaystyle\int_0^T (\boldsymbol{E}^i \times \boldsymbol{H}^{i*})\cdot(-\boldsymbol{y})\, dx} \tag{17}$$

where $\boldsymbol{E}_n^r, \boldsymbol{H}_n^r, \boldsymbol{E}_n^t$, and $\boldsymbol{H}_n^t$ are the reflected and transmitted fields for mode n. $\boldsymbol{E}^i, \boldsymbol{H}^i$ are the incident fields and $\boldsymbol{y}$ is the unit vector along the y axis.

III. Numerical Results

We considered silicon to be the substrate of the metallic strip grating structures in numerical calculations. The material constants of silicon are $\varepsilon_s = 11.8, m_e = 0.259 \times m_0$ [kg], $m_h = 0.380 \times m_0$ [kg], $m_0 = 9.11 \times 10^{-31}$ [kg], $\nu_e = 4.52 \times 10^{12}$ [s^{-1}], $\nu_h = 7.71 \times 10^{12}$ [s^{-1}] [1]. We assumed that the thickness of the optically induced plasma layer was $t_p = 20$ μm [2]. The surface resistance R of the metallic strips is 0 Ω. In calculations of (16), we set the absolute value N of the upper and lower limit of n at 100 or more (the number of the mode expansion $2N+1$ was set at 201 or more). The number of the basis functions M of the surface current in (14) was 11. A satisfactory convergence of the solution was assured with this number of the expansion modes and these basis functions.

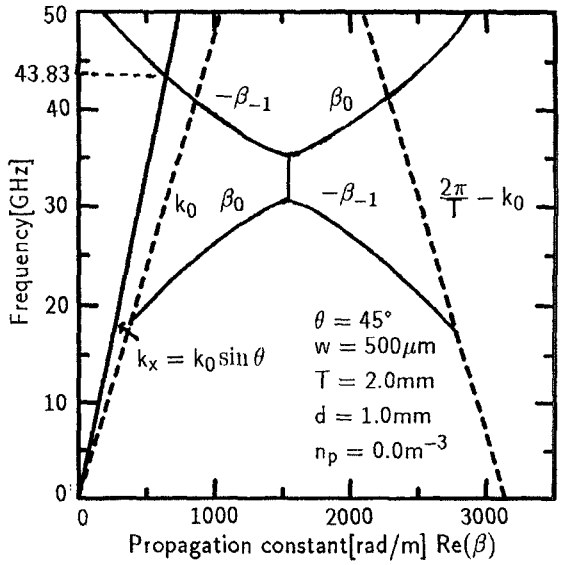

Fig. 2. Transverse wavenumber $k_x = k_0 \sin\theta$ of the incident plane wave and the dispersion curves of a TE surface wave in the silicon slab waveguide with metallic strip gratings.

In Figs. 2–4, we show numerical calculations for the silicon thickness of $d = 1.0$ mm, the period of $T = 2.0$ mm, and the strip width of $w = 500$ μm. Fig. 2 shows the transverse wave number $k_x = k_0 \sin\theta$ of the incident plane wave and the real part of the propagation constant Re(β), with which TE surface waves propagate in the silicon slab waveguide with the metallic strip gratings, but without induced plasma ($n_p = 0.0$ m^{-3}). β was calculated by the spectral domain method [10], [11]. From this figure we found that, near $f = 43.83$ GHz in the leaky wave region, the transverse wave number curve of the plane wave $k_x = k_0 \sin\theta$ for the angle of incidence $\theta = 45°$ intersects the dispersion curve $-\beta_{-1}$ of the $n = -1$ space harmonic of the surface wave mode travelling in the $-x$ direction in Fig. 1. We expected that, in the vicinity of this frequency, the plane wave of $n = 0$ will couple with the $n = -1$ space harmonic, and Wood's anomalies will occur [12], [13]. Fig. 3 shows the frequency dependence of power reflection coefficients of (17) as a function of plasma density n_p. As mentioned above sharp notch filter, characteristics were caused by the resonance anomaly near $f = 43.83$ GHz. As the plasma density n_p increased, the resonant frequency shifted slightly to a higher frequency, while shifting to a lower frequency for TM wave [6]. We also found that when the plasma density n_p was 1.0×10^{23} m^{-3}, the incident plane wave was completely reflected, because the optically induced plasma layer in the silicon functions almost as a perfect conductor. Fig. 4 shows the incident angle dependence of power reflection coefficients as a function of plasma density at $f = 43.83$ GHz. The sharp notch filter characteristic was caused by the resonance anomaly around $\theta = 45°$. As plasma density n_p increased, the incident angle at which the resonance occured increased, while the incident angle decreased for the TM wave [6].

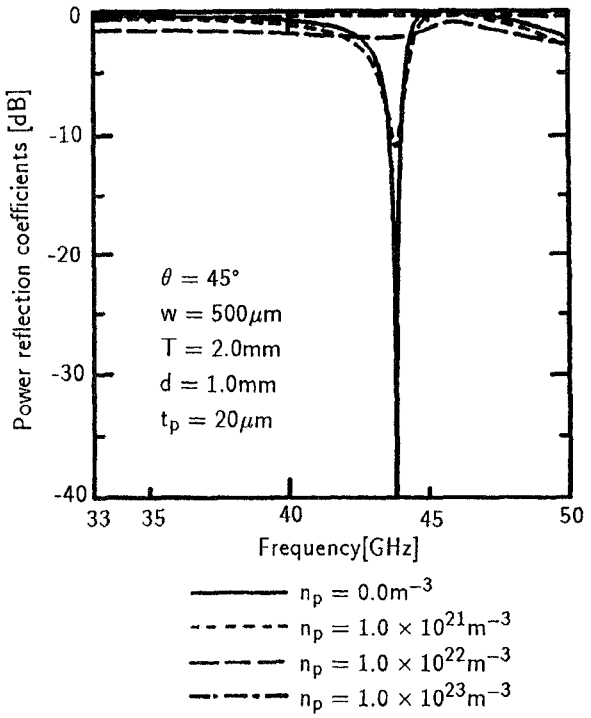

Fig. 3. Frequency dependence of power reflection coefficients as a function of plasma density.

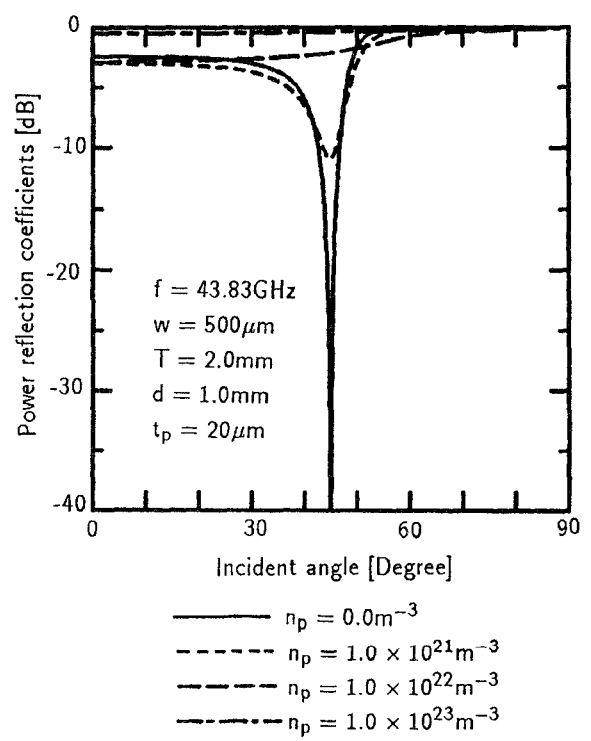

Fig. 4. Incident angle dependence of power reflection coefficients as a function of plasma density.

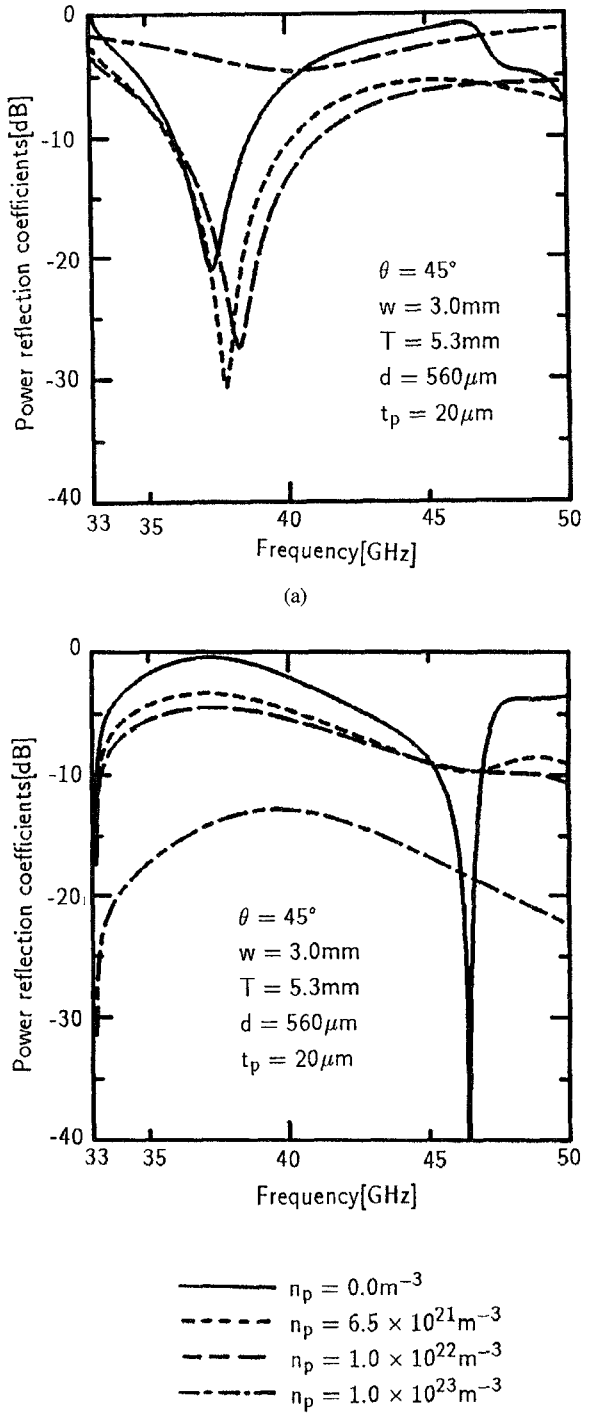

Fig. 5. Frequency dependence of power reflection coefficients for blazing effect as a function of plasma density. (a) Zero-order mode. (b) −1-order mode.

In Fig. 5, numerical calculations of the power reflection coefficients were carried out for a silicon thickness of $d = 560\ \mu$m, a period of $T = 5.3$ mm, a strip width of $w = 3.0$ mm, and an incident angle of $\theta = 45°$. Fig. 5(a) and (b) shows the frequency dependence of the zero and -1 order power reflection coefficients as a function of plasma density n_p. At $n_p = 0.0\ \text{m}^{-3}$ in Fig. 5(a), the zero-order reflected wave is seen to be suppressed to a power level under -20 dB in a frequency band from 37.09–37.47 GHz, due to the blazing effect [14], [15]. This corresponds to -0.43 dB for the power conversion from the incident wave to the -1-order refleced wave. The blazing effect is the power conversion from the incident plane wave to the -1-order diffracted wave

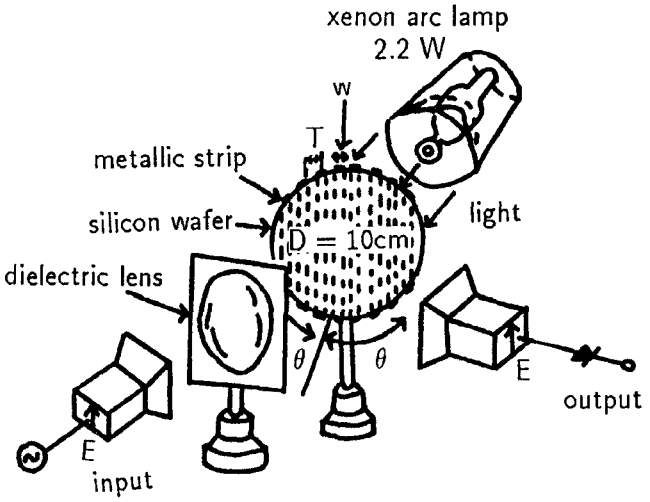

Fig. 6. Experiment on quasi-optical grating circuits using silicon wafer.

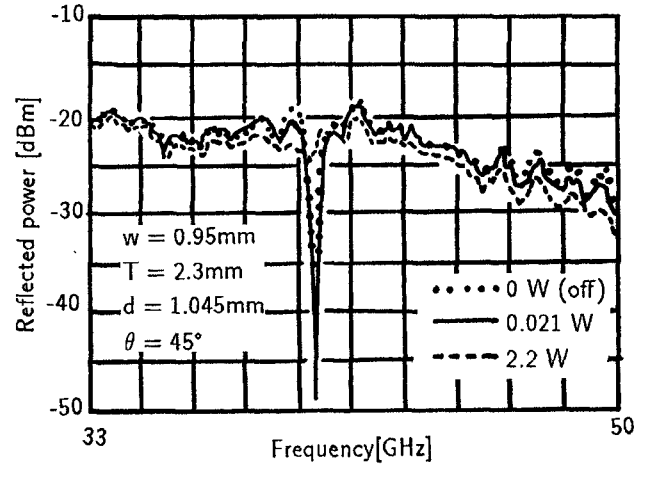

(a)

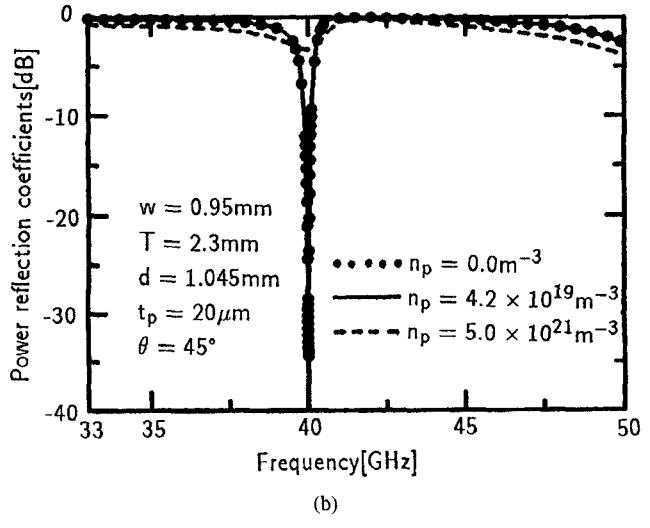

(b)

Fig. 7. Frequency dependence of the zero-order reflected power as a function of optical power. (a) Measured zero-order reflected power. (b) Calculated zero-order power reflection coefficients.

and was optimized for the computations shown in Fig. 5 by the structure parameters of the grating: the thickness of the substrates, the strip width, the periodicity of the grating, and the Bragg condition, $\sin\theta = \lambda_0/2T$ [14], [15]. The blazing

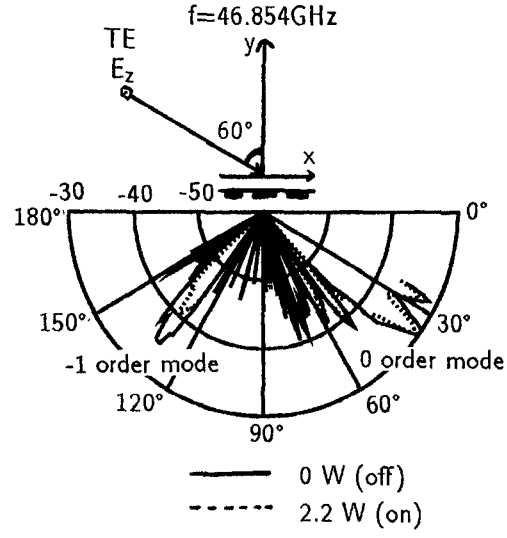

Fig. 8. Measured optical control characteristics of forward scattering pattern.

effect is applied to frequency-scanning antennas because the propagation direction of the higher-order diffracted wave is frequency-dependent. As the plasma density n_p increases, the frequency giving the minimum value of the zero-order power reflection coefficients, which is 37.28 GHz at $n_p = 0.0\ \mathrm{m}^{-3}$, shifts to the higher frequency. The zero-order power reflection coefficients become minimum at $n_p = 6.5 \times 10^{21}\ \mathrm{m}^{-3}$, as seen in Fig. 5. The higher the plasma density n_p, the more the -1-order reflected wave attenuates for whole frequency range. For $n_p = 10^{23}\ \mathrm{m}^{-3}$, the metallic strip gratings are shortened and have no effect on the gratings because the plasma layer approaches an almost perfect conductor state.

IV. Experimental Results

Fig. 6 shows the experiment situation. Two types of metallic strip grating structures were fabricated on a highly resistive silicon wafer, with a resistance of more than 5 $\mathrm{k}\Omega \cdot \mathrm{cm}$ and a 100 mm diameter. The parameters of the grating structures were

Grating Structure I:
- d (silicon thickness) = 1.045 mm
- T (period of the grating) = 2.3 mm
- w (metallic strip width) = 0.95 mm
- number of metallic strips = 40

Grating Structure II:
- $d = 400\ \mu\mathrm{m}$
- $T = 4.2$ mm
- $w = 1.8$ mm
- number of metallic strips = 19.

A surface without grating structures was illuminated by a TE wave through a 7.5-cm-caliber dielectric lens. The grating structures were illuminated by a xenon arc lamp with an optical output of 2.2 W. The scattering characteristics of the grating structures of a TE wave were measured over a frequency of 33–50 GHz, with a fixed incident angle of the TE wave (Fig. 6).

To examine the effect of the light illumination on the resonance anomaly, we measured the power of the zero-order

reflected wave from grating structure I. The distances between the grating structure and the transmitting and receiving horns were 17 cm and the distance between the transmitting horn and the dielectric lens was 8 cm. Fig. 7(a) shows the measured power of the zero-order reflected wave from the grating structure illuminated by a TE wave with an incident angle $\theta = 45°$. Fig. 7(b) shows the calculated results of the zero-order power reflection coefficients, where the parameters of the grating structure used for our calculations were the same as those in the experiment in Fig. 7(a). In the results of Fig. 7(a), the notch filter characteristic near 40.31 GHz was caused by a resonance anomaly. The resonant frequency was about 310 MHz higher than theoretically predicted. The measured notch attenuation, excepting insertion loss of -20 dB is close to 16.4 dB for optical power of 0 mW, smaller than the calculated notch attenuation 34.5 dB for $n_p = 0.0\ \mathrm{m}^{-3}$ in Fig. 7(b). The measured notch attenuation, excepting the insertion loss is close to 27.8 dB for an optical power of 21 mW and shows the maximum notch as depicted in $n_p = 4.2 \times 10^{19}\ \mathrm{m}^{-3}$ in Fig. 7(b). The measured notch attenuation for an optical power of 2.2 W, expecting the insertion loss, is approximately 3 dB and is similar to the calculated notch attenuation of 2.6 dB for $n_p = 5.0 \times 10^{21}\ \mathrm{m}^{-3}$ in Fig. 7(b). The discrepancy between theory and experiment is primarily attributable to the high tan δ value of the silicon wafer and the Gaussian distribution of the TE plane wave, which are neglected in theory. Thus, it seems that the measured dependence of the notch attenuation on the optical control is similar to the computed characteristics in Fig. 7(b). Throughout our experiments, the density of the plasma induced by the light of optical output 2.2 W was presumed to be $n_p \simeq 5.0 \times 10^{21}\ \mathrm{m}^{-3}$ and $n_p t_p \simeq 1.0 \times 10^{17}\ \mathrm{m}^{-2}$. This presumed plasma density is the same order as the plasma density reported in previous work [2], [6].

Next, the optical control characteristics of the forward scattering pattern for grating structure II were measured for a TE wave incident at an angle $\theta = 60°$ and having $f = 46.854$ GHz. The scattering was measured by rotating the receiving horn antenna from 25–155° and is shown in Fig. 8. The distances of the grating structure II from the transmitting and receiving horns were 27 cm, and the distance between the transmitting horn and the dielectric lens was 13 cm. For an optical output of 0 W, the lobe of the zero-order transmitted wave was observed at 36° and the lobe of the -1-order transmitted wave observed at 131°. As predicted in theory, when the frequency sweeps from 41.6–46.9 GHz, a 20° frequency scanning of the lobe of the -1-order transmitted wave, from 151–131°, was observed. The plasma density dependence of the forward scattering pattern was calculated for the same parameters used in Fig. 8. The difference of the lobe of the zero-order transmitted wave with and without an optical power of 2.2 W is 1.04 dB in the experiment depicted in Fig. 8; the difference in the zero-order power transmission coefficient at $n_p = 0.0\ \mathrm{m}^{-3}$ and $n_p = 1.3 \times 10^{21}\ \mathrm{m}^{-3}$ was 1.039 dB in theory. While the difference of the lobe of the -1-order transmitted wave with and without an optical power of 2.2 W is 5.29 dB in the experiment in Fig. 8, the difference of the -1-order power transmission coefficient at $n_p = 0.0\ \mathrm{m}^{-3}$ and $n_p = 5.6 \times 10^{21}\ \mathrm{m}^{-3}$ was 5.28 dB in theory. Thus, the density of plasma density induced by the light of 2.2 W was roughly estimated to lie between $n_p = 1.3 \times 10^{21}\ \mathrm{m}^{-3}$ and $n_p = 5.6 \times 10^{21}\ \mathrm{m}^{-3}$ ($n_p t_p$ between $2.6 \times 10^{16}\ \mathrm{m}^{-3}$ and $1.12 \times 10^{17}\ \mathrm{m}^{-3}$). This density, presumed from the forward scattering patterns of grating structure II, is the same order as the plasma density presumed from the measured zero-order reflection characteristics of grating structure I.

V. Conclusion

We have analyzed the scattering characteristics of a TE electromagnetic plane wave by using metallic strip gratings on an optically induced plasma in a semiconductor, utilizing the spectral domain Galerkin method. We have explained the effect of the optically induced plasma on the scattering characteristics of the TE electromagnetic plane wave through a numerical technique. From the numerical calculation of the reflection characteristics, we found that when the plasma is induced optically in a semiconductor, the frequency and incident angle at which the resonance occurs increase. Two types of metallic strip gratings on highly resistive silicon were fabricated and were used to measure the frequency dependence of the zero-order reflected power, and the forward scattering pattern and diffracted wave from the gratings over a frequency band from 33–50 GHz. Throughout the experiments, we demonstrated that the resonance anomaly and the forward scattering pattern could be controlled by the light illumination, as discussed in the theory. The experimental results do not, however, demonstrate as great an optical control as predicted theoretically, due to the high tan δ value of silicon wafer.

The characteristics shown in this paper will be the basis for designing and studying new circuit elements designated as optical control of quasioptical circuits and devices, such as filters and frequency scannable antennas at submillimeter-wave frequencies.

References

[1] "Special Issue on Applications of Lightwave Technology to Microwave Devices, Circuit and System," *IEEE Trans. Microwave Theory Tech.* vol. 38, no. 5, May 1990.

[2] K. Nishimura and M. Tsutusmi, "Optical control of the printed dipole antenna," *Trans. IEICE of Japan*, vol. J78-C-I, no. 3, pp. 173–179, Mar. 1995.

[3] S. Sugiyama and M. Tsutusmi, "Reflection and transmission of millimeter waves from the plasma induced semiconductor slab," *Trans. IEICE of Japan*, vol. J73-C-I, no. 4, pp. 173–178, Apr. 1990.

[4] G. Degado, J. Johansson, A. Larsson, and T. Andersson, "Optical controlled spatial modulation of (sub-)millimeter waves using *nipi*-doped semiconductors," *IEEE Microwave Guided Wave Lett.*, vol. 5, no. 6, pp. 198–200, June 1995.

[5] V. A. Manasson, L. S. Sadovnik, A. Moussesian, and D. B. Rutledge, "Millimeter-wave diffraction by a photo-induced plasma grating," *IEEE Trans. Microwave Theory Tech.*, vol. 43, no. 9, pp. 2288–2290, Sept. 1995.

[6] K. Nishimura and M. Tsutsumi, "Optical control of milllimeter waves of quasi optical grating structures," Tech. Rep. IEE Japan, EMT-95-12, Jan. 1995 (in Japanese).

[7] R. C. Hall and R. Mittra, "Scattering from a periodic array of resistive strips," *IEEE Trans. Antennas Propagat.*, vol. AP-33, no. 9, pp. 1009–1011, Sept. 1985.

[8] K. Uchida, T. Noda, and T. Matsunaga, "Spectral domain analysis of electromagnetic wave scattering by an infinite plane metallic grating," *IEEE Trans. Antennas Propagat.*, vol. AP-35, no. 1, pp. 46–52, Jan. 1987.

[9] J. L. Volakis, Y. C. Lin, and H. Anastassiu, "TE characterization of resistive strip gratings on a dielectric slab using a single edge mode expansion," *IEEE Trans. Antennas Propagat.*, vol. AP-42, no. 2, pp. 203–212, Feb. 1994.
[10] J. Jacobsen, "Analytical, numerical, and experimental investigation of guided waves on a periodically strip-loaded dielectric slab," *IEEE Trans. Antennas Propagat.*, vol. AP-18, no. 3, pp. 379–388, May 1970.
[11] K. Ogusu, "Propagation properties of a planar dielectric waveguide with periodic metallic strips," *IEEE Trans. Microwave Theory Tech.*, vol. MTT-29, no. 1, pp. 16–21, Jan. 1981.
[12] H. L. Bertoni, L. S. Chen, and T. Tamir, "Frequency-selective reflection and transmission by a periodic dielectric layer," *IEEE Trans. Antennas Propagat.*, vol. AP-37, no. 1, pp. 78–83, Jan. 1989.
[13] R. Magnusson, S. S. Wang, T. D. Black, and A. Sohn, "Resonance properties of dielectric waveguide gratings: theory and experiments at 4–18 GHz," *IEEE Trans. Antennas Propagat.*, vol. 42, no. 4, pp. 567–569, Apr. 1994.
[14] F. S. Johansson, L. G. Josefsson, and T. Lorentzon, "A novel frequency-scanned reflector antenna," *IEEE Trans. Antennas Propagat.*, vol. 37, no. 8, pp. 984–989, Aug. 1989.
[15] F. S. Johansson, "Frequency-scanned gratings consisting of photo etched arrays," *IEEE Trans. Antennas Propagat.*, vol. 37, no. 8, pp. 996–1002, Aug. 1989.

Kazuo Nishimura (S'77–M'79) was born in Kyoto, Japan, on December 26, 1967. He received the B.E. degree in electrical engineering and the M.E. degree in electronics and information engineering from Kyoto Institute of Technology, Kyoto, Japan, in 1991 and 1993, respectively. Since 1993, he has been pursuing the Ph.D. degree in the Department of Electronics and Information Science at Kyoto Institute of Technology, where he has been engaged in millimeter-wave waveguides, electromagnetic absorbers, and microstrip antennas. His current interests are optically controllable microwave and millimeter-wave devices.

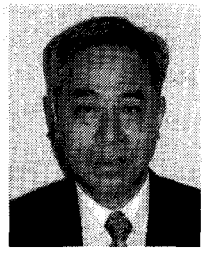

Makoto Tsutsumi (M'71) was born in Tokyo, Japan, on February 25, 1937. He received the B.S. degree in electrical engineering from Ritsumeikan University, Kyoto, Japan, in 1961 and the M.S. and Ph.D. degrees in communication engineering from Osaka University, Osaka, Japan, in 1963 and 1971, respectively.

From 1984 to 1987, he was an Associate Professor of Communication Engineering, Osaka University. Since 1988, he has been a Professor, Department of Electronics and Information Science, Kyoto Institute of Technology. His research interests are primarily in microwave and millimeter-wave ferrite devices and optics/microwave interactions in the semiconductor.